Weakly Nonlinear Gas Oscillations in Air-Filled Tubes; Solutions and Experiments

Ludovic Menguy, Joël Gilbert

Article project to Acta Acustica

Date:	23-08-2000
Title:	**Weakly nonlinear gas oscillations in air-filled tubes; solutions and experiments.**
Authors:	Ludovic MENGUY, Joël GILBERT
	Laboratoire d'Acoustique de l'Université du Maine (UMR CNRS 6613)
	Av. O. Messiaen, 72085 Le Mans cedex 9, France.
Author to contact:	Dr. Joël Gilbert
Phone number:	(33) 2 43 83 32 83
Fax number:	(33) 2 43 83 35 20
E-mail:	joel.gilbert@univ-lemans.fr

Contents

Nonlinear acoustic propagation in cylindrical air-filled tubes; solutions and experiments

Ludovic MENGUY, Joël GILBERT

Laboratoire d'Acoustique de l'Université du Maine (UMR CNRS 6613)

Avenue O. Messiaen, 72085 Le Mans cedex 9, France.

Summary

The results of a theoretical and experimental investigation into the nonlinear, planar propagation of an acoustic signal in a cylindrical air-filled tube is presented. Assuming weakly nonlinear propagation and the distance of propagation smaller than the shock formation distance, the validity of the generalised Burgers' equation is analysed. The theoretical study is based on a dimensional analysis of the conservation equations followed by a calculation using asymptotic expansions. The deduced generalised Burgers' equations are solved *whatever* the boundary conditions are, with a numerical finite-difference method and using a harmonic balance method. Two cases are investigated experimentally: the purely progressive case, and the standing wave with an unknown termination. The results are compared successfully with theoretical predictions on the three first harmonics of a periodic signal in a high degree of accuracy, when the effects of the thermoviscous dissipation and of the non-linear propagation have the same order of magnitude.

Keywords: nonlinear acoustic propagation, boundary layer losses, standing waves, cylindrical guide.

1 Introduction

For small amplitude disturbances, the plane wave deformation during propagation in an acoustic wave guide is mainly controlled by thermoviscous losses in the wall boundary layers. In the last century, Kirchhoff [1] proposed a description of linear sound propagation in guides. From this work Zwickker & Kosten [2] obtained a general solution of the problem in ω-space including both absorption and dispersion due to these

thermoviscous effects along the tube walls.

It is well known that for high amplitude disturbances, the acoustic wave can be highly distorted [3] [4] leading to shock formation (see for example the unexpected shock waves observed in musical brass instruments, Hirschberg et al [5], Gilbert and Petiot [6]). These kind of spectacular effects cannot be explained with linear acoustic approximations. The present works deals with weakly nonlinear acoustic propagation (acoustic velocity much smaller than the speed of the sound) in cylindrical air-filled tubes.

Local small nonlinear perturbations of the acoustic wave due to high sound levels are cumulative along the propagation and may distort the wave form considerably at sufficiently large distances. Work in nonlinear propagation in free space has previously been subjected to extensive investigations because of research in underwater acoustics using ultrasound or more recently bioacoustics. We can cite Whitham [7], Kuznetsov [8], Blackstock [9], Rudenko & Soluyan [10]. Coulouvrat [11] presents an exhaustive review of works concerning the propagation of an acoustic beam in a thermoviscous fluid. The nonlinear propagation of a plane wave (uni-dimensional propagation) in a perfect fluid is solved with the method of Riemann invariants. Taking into account volumetric losses leads to a description of the wave in the neighbourhood of the shock.

In ducts, theoretical foundations of nonlinear wave propagation with wall friction can be found in Chester [12]. He derived nonlinear equations and solved them using a perturbation method. Nonlinear equations are usually solved for specific cases, e.g., progressive waves (Pernet & Peyne [13], Sugimoto [14]); closed tube with a rigid termination (Chester [12]) or open tubes (Chester [15]). The aim of our study is to solve the nonlinear equations in a tube not only in specific cases but with any periodic source and any termination.

A classical perturbation method can lead to unsatisfactory results because of cumulative effects: a small local phenomenon can become perceptible at sufficiently large distances. A good description of cumulative effects is obtained using a Multiple Scale Method (MSM), which separates non cumulative effects remaining negligible, and cumulative effects. This leads to generalized Burgers' equations. The effect of boundary layer losses is taken into account by a convolution product (Blackstock [9]) which can be formally written with a fractional derivative (Blackstock [16], Sugimoto [14]).

Experiments in tubes were performed by Cruikshank [17] in a closed tube (results are compared with

Chester's theory [12]), Sturtevant [18] (closed and open tubes) and Zaripov & Ilhamov [19] (closed tubes, higher oscillations). Gaete-Garreton & Gallego-Juarez [20] studied the progressive wave. More recent experiments were performed by Maa & Liu [21] in closed tubes.

The objective of this work is to give solutions of a standing weakly nonlinear acoustic wave propagating in a cylindrical guide, filled with a thermo-viscous fluid (air), with a good accuracy, within a certain validity domain (see figure), /textit[whatever] the boundary conditions and not only closed tubes or open tubes or sinusoidal sources. At our knowledge, this has not been done before in such extensive cases. Boundary conditions at one end are acoustic pressure or velocity (a periodic signal which is not necessarily sinusoidal) and impedance or acoustic signal at the other end. In a first part, hypotheses and approximations are studied. The order of magnitude of all variables as well as their spatial variations are discussed. The validity domain of each approximation is studied. This will be useful to verify the agreement between the validity domain of the theoretical solutions obtained and experiments performed (typically frequencies of the order of 1kHz, a radius of the order of 1cm and sounds levels around 150dB). Equations of conservation (mass, momentum and energy) are then written and rendered dimensionless separately in the acoustic boundary layer and in the main acoustic flow. Dimensionless numbers appear in front of each term in the equations and are characteristic of the order of magnitude of the corresponding terms. A perturbative calculation using asymptotic expansions is then performed. Equations are simplified and averaged over a cross section of the main acoustic field of the tube. An asymptotic matching with the boundary layer is then performed, leading to nonlinear propagation equations similar to these obtained by Chester [12]. The application of the Multiple Scale Method leads to two Burgers' equations in the case of a standing wave. These two Burger's equation are independent of each other: it is possible to consider the standing wave as the sum of two independent progressive waves. Each progressive wave is governed by one of the independent Burgers' equations. This is obtained because the interaction between the two progressive waves exists locally, but according to the MSM it does not cumulate, and therefore stays negligible. This is a new and original result, not obtained before to our knowledge. Resolution of these Burgers' equations is performed numerically from two boundary conditions (impedance or signal imposed) at both ends of the tube. A harmonic balance

method (Newton-Raphson) is used to calculate the two traveling waves. The signal at any point in the tube is then deduced and compared with experiments (see also Menguy et al. [22]). The discrepancy between theory and experiments is of order 0.1dB for the fundamental and the harmonic number 2, and within 0.5dB for the harmonic 3.

2 From the fundamental equations to the nonlinear equations of acoustic propagation

2.1 Hypotheses and dimensional analysis

The motion of a classical fluid is governed:

-by the conservation laws (mass, momentum, and energy conservation);

-by relations and conditions who specify the mechanical and thermodynamical properties of the fluid;

-by the geometry and boundary conditions.

The fundamental conservation equations are as follows (see for example Landau & Lifschitz [23], Rudenko & Soluyan [10], Batchelor [24]).

The conservation of mass is:

$$\frac{\partial \tilde{\rho}}{\partial \tilde{t}} + div(\tilde{\rho}\,\vec{\tilde{u}}) = 0; \tag{1}$$

the conservation of momentum is:

$$\tilde{\rho}\frac{d\vec{\tilde{u}}}{d\tilde{t}} = -\overrightarrow{grad}\tilde{P} + (\eta + \frac{1}{3}\mu)\overrightarrow{grad}(div\,\vec{\tilde{u}}) + \mu\vec{\triangle}\,\vec{\tilde{u}}; \tag{2}$$

and assuming the heat flux satisfies the Fourier law, the conservation of energy is:

$$\tilde{\rho}\tilde{T}\frac{d\tilde{S}}{d\tilde{t}} = F_d + k_h\triangle\tilde{T}. \tag{3}$$

F_d is the rate of dissipation of mechanical energy of the fluid. μ, η, ν, k_h, c_0, λ and ω denote respectively the first and second viscosities, the kinematic viscosity, the thermal conductivity, a typical value of the speed of the sound in air, the wavelength and the acoustic angular frequency. $\vec{u}$ is the particle velocity, $\tilde{S}$ the

specific entropy, $\tilde{T}$ the temperature, $\tilde{P}$ the pressure and $\tilde{\rho}$ the volumic density.

Properties of the fluid are as following. The fluid (air) is newtonian, in the laminar regime, in steady state and is considered as a perfect gas (the fluid is bivariant). Heat exchange satisfies the Fourier law. Relaxation phenemenon are neglected. The plane wave assumption is adopted.

The problem is axisymmetric. The axis (Ox) is aligned along the tube axis and (Or) along the radius. The axial and radial components of the acoustic velocity $\vec{\tilde{u}_a}$ are denoted $\tilde{u}_a$ and $\tilde{v}_a$ respectively. The wall of the tube is supposed rigid and conducts heat perfectly; non slip condition is assumed along the walls. On the wall, velocities and acoustic temperature are therefore equal to zero. These conditions create large gradients of acoustic temperature and velocities close to the wall; this region is called the boundary layer. The thickness of the viscous boundary layer is $\xi = \sqrt{\nu/\omega}$ and the ratio of the thickness of the viscous and the thermal boundary layers is $Pr^{1/2}$ with $Pr = (\mu Cp)/(k_h)$ the Prandtl number, which is of order unity ($Pr \simeq 0.7$ for the air; C_p is the specific heat at constant pressure). The two regions (boundary layer and the rest of the tube called main acoustic field) are studied separately.

The dimensional analysis relies on the existence of three dimensionless numbers which are much less than unity:

$$M = \frac{\tilde{u_{a0}}}{c_0} \ll 1 \quad ; \quad \frac{1}{Re} = \frac{\nu\omega}{c_0^2} \ll 1 \quad ; \quad Sh = \frac{\xi}{R} = \sqrt{\frac{\nu}{\omega}}\frac{1}{R} \ll 1.$$

M is the acoustic Mach number, Re the acoustic Reynolds number, and Sh the Shear number (see for example Disselhorst & Van Wijngaarden [25]) , the ratio of the boundary layer thickness ξ and the tube radius R (using the large tube radius approximation). $\tilde{u_{a0}}$ is a typical value (constant) of the acoustic velocity (for example the velocity of the fundamental component near the source).

The conditions which motivate our study relate to frequencies in the audible range, radii of order a centimeter, and high sound levels (140-160dB). It can thus be assumed that $1/Re$ is around three orders of magnitude smaller than M and Sh:

$$M^2 Re = \frac{\tilde{u}_a^2}{\nu\omega} \gg 1 \quad \text{and} \quad Sh^2 Re = (\frac{c_0}{R\omega})^2 \gg 1.$$

The second condition reflects the fact that the wavelength is large in comparison with the tube radius. Then the plane wave approximation is easily verified:

$$\frac{R}{\lambda} < 0.29.$$

The former two conditions imply that

$$MRe = \frac{\tilde{u}_a^2}{\nu\omega} \gg 1 \quad \text{and} \quad \frac{1}{ReSh} = \sqrt{\frac{\omega\mu}{\rho_0 c_0^2}}\frac{\omega R}{c_0} \ll 1.$$

This last condition means that thermoviscous effects are only boundary layer effects and not volumetric losses.

The hypotheses can be summarized as follows:

$$1 \gg M, Sh \gg M^2, Sh^2, MSh \gg 1/Re, M^3, M^2Sh, MSh^2, Sh^3. \tag{4}$$

These orders of magnitude are denoted order 0, 1, 2 and 3 respectively in the following text.

FIGURE 1. Validity domain

A predominance diagram (see figure 1) is used to verify the validity domain. The tube radius is imposed at 3cm (our experimental conditions) and the competition between different terms is represented on a logarithmic scaled graph, pressure [dB] on y-scale and frequency on x-scale. For example the line $M^2 = Sh$ means that above this line M^2 is predominant compared to Sh, and conversely under. A first order theory on M and Sh is optimal only under this line but not above. Nonlinear second order phenomenon should be much more important than thermoviscous boundary layer losses above this line, and then the classical exact nonlinear theory for a plane wave in a perfect fluid (Riemann invariants) would be more precise. Lines $M = 1/(ReSh)$ and $M = Sh^2$ indicate the limit under which a nonlinear theory is not useful because nonlinear phenomena are negligible compared to other linear phenomena neglected, such as the effect of the curvature of the boundary layer or the effect of volumetric losses, for example. Lastly, the Merkly condition ($\tilde{u}/\sqrt{\nu\omega} < 350 - 700$) to have a laminar acoustic boundary layer is valid under the line represented.

All these conditions are valid in a certain zone (see figure 1), and all experimental mesurements are placed

on this graph to verify the validity of the hypotheses.

The fundamental equations (conservation of mass and momentum) are expressed in cylindrical coordinates, since the problem is axisymmetric. The equations are simplified separately in the boundary layer and in the main acoustic field by considering the order of magnitude of each term. For that purpose the equations are converted into a dimensionless form. The aim is to rewrite each term in the form of a variable of order 1, preceded by a dimensionless number characterising the order of magnitude of the term studied. The acoustic quantities are locally of order M. The following changes of variables are made respectively in the main acoustic field, respectively in the boundary layer. Dimensional and dimensionless variables are written respectively with tilde and without tilde in the following text.

$$\begin{array}{llllll}
\tilde{\rho} & \text{becomes} & \tilde{\rho} = \rho_0(1 + M\rho_a), & \text{respectively} & \tilde{\rho} = \rho_0(1 + M\rho_{ab}); \\
\tilde{P} & \text{becomes} & \tilde{P} = P_0(1 + MP_a), & \text{respectively} & \tilde{P} = P_0(1 + MP_{ab}); \\
\tilde{T} & \text{becomes} & \tilde{T} = T_0(1 + MT_a), & \text{respectively} & \tilde{T} = T_0(1 + MT_{ab}); \\
\tilde{u} & \text{becomes} & \tilde{u} = c_0(Mu_a), & \text{respectively} & \tilde{u} = c_0(Mu_{ab}); \\
\tilde{S} & \text{becomes} & \tilde{S} = S_0 + MR_gS_a, & \text{respectively} & \tilde{S} = S_0 + MR_gS_{ab}.
\end{array}$$

ρ_0, P_0 are the static values of $\tilde{\rho}$ and $\tilde{P}$ in the absence of an acoustic field. Every indexed dimensionless variable is of order unity by definition. Only S_a is not necessarily of order of unity (it will be pointed out in the main acoustic field in the following text) and is therefore noted between $\langle\rangle$ to differentiate it from other terms.

The dimensional analysis of the radial components $\tilde{v}_a$ and $\partial/\partial r$ is not straightfoward. Their order of magnitude can be obtained from the linear results:

$$\tilde{v} \quad \text{becomes} \quad \tilde{v} = \frac{c_0}{\sqrt{Re}} M v_a.$$

Moreover, there are three different orders of magnitude among the spatial variables. Thus $(\tilde{x})$ is set dimensionless using c_0/ω, and $(\tilde{r})$ using R (denoted r_1) or ξ (denoted r_{b1}) respectively in the main acoustic field and the boundary layer.

A further problem is to render dimensionless the spatial derivatives. The gradients with respect to r of the variables in the tube are not all of the same order. In the boundary layer, for example, u_a varies from 0 at

the wall to a velocity of order of Mc_0 (the acoustic velocity in the main field) far from the wall: $\partial \tilde{u_a}/\partial \tilde{r}$ is thus of order of $\tilde{u_a}/\xi$, while $\partial \tilde{T_a}/\partial \tilde{r}$ and $\partial \tilde{v_a}/\partial \tilde{r}$ are of order $\tilde{T_a}/\xi$ and $\tilde{v_a}/\xi$ respectively. $v_a = 0$ on the axis of the tube because of axisymetry of the tube: therefore $\partial \tilde{v_a}/\partial \tilde{r}$ is of order $(\tilde{v_a}/R)$ in the main acoustic field. But notice that the order of magnitude of $\partial X/\partial Y$ is not necessarily the same as that of X/Y: for example the acoustic pressure varies little over the cross-section of the tube. The order of magnitude of $\partial \tilde{P_a}/\partial \tilde{r}$ is not $\tilde{P_a}/R$ but much less. The results of linear acoustics guided our choice for the derivatives of quantities. Radial derivatives are set dimensionless. Taking into account the actual radial variation of variables in rendering equations dimensionless is where the present work differs from Chesters. Doing so improves the validity of the perturbation method compared with using only ξ in the boundary layer and R in the main acoustic field. In the boundary layer

$$\frac{\partial}{\partial \tilde{r}} \quad \text{becomes} \quad \frac{1}{\xi}\frac{\partial}{\partial r_{b1}} = \sqrt{\frac{\rho_0 \omega}{\mu}}\frac{\partial}{\partial r_{b1}} \qquad \text{applied to} \quad T_a, S_a, \rho_a, u_a, \text{ and } v_a,$$

$$\frac{\partial}{\partial \tilde{r}} \quad \text{becomes} \quad \frac{1}{Re}\frac{1}{\xi}\frac{\partial}{\partial r_{b2}} = \frac{1}{Re}\sqrt{\frac{\rho_0 \omega}{\mu}}\frac{\partial}{\partial r_{b2}} \quad \text{applied to} \quad P_a,$$

and in the main acoustic field

$$\frac{\partial}{\partial \tilde{r}} \quad \text{becomes} \quad \frac{1}{R}\frac{\partial}{\partial r_1} \qquad \text{applied to} \quad v_a,$$

$$\frac{\partial}{\partial \tilde{r}} \quad \text{becomes} \quad \frac{1}{Re}\frac{1}{\xi}\frac{\partial}{\partial r_{b2}} = \frac{1}{Re}\sqrt{\frac{\rho_0 \omega}{\mu}}\frac{\partial}{\partial r_{b2}} \quad \text{applied to} \quad T_a, S_a, P_a, \rho_a, \text{ and } u_a.$$

$$\text{with} \quad r_1 = \frac{\tilde{r}}{R}, \quad r_{b1} = \frac{\tilde{r}}{\xi} \quad \text{and} \quad r_{b2} = \frac{\tilde{r}}{Re\xi}$$

Then, conservation laws (1), (2) and (3) are written dimensionless in cylindrical coordinates, both in the boundary layer and in the main acoustic field. The order of magnitude of each term is therefore given explicitely by a dimensionless number. It becomes easy to justify the reason why one term or one effect should be neglected or not. Equations can therefore be rigorously simplified, and the order of magnitude of each neglected term is known. Obtained equations are then solved in the boundary layer and matched asymptotically with the main acoustic field. An averaging across a section of the tube leads to two non linear equations (see appendix A).

2.2 Nonlinear equations of propagation

The setting of the nonlinear equations with only two variables u_a and ρ_a leads to (see appendix A, and equations (59) and (60)):

$$\frac{\partial \rho_a}{\partial t} + \frac{\partial}{\partial x}\big((1+M\rho_a)u_a\big) - 2Sh\Big(1+\frac{\gamma-1}{\sqrt{Pr}}\Big)\frac{\partial u_a}{\partial x} * \frac{1}{\sqrt{\pi t}} = O\big(MSh, Sh^2, \frac{1}{ReSh}\big), \tag{5}$$

$$\frac{\partial u_a}{\partial t} + Mu_a\frac{\partial u_a}{\partial x} + (1+M\rho_a)^{\gamma-2}\frac{\partial \rho_a}{\partial x} = O\big(\frac{1}{ReSh}\big). \tag{6}$$

Notice that if the variable

$$c = (1+M\rho)^{\frac{\gamma-1}{2}} \tag{7}$$

is introduced, multiplying (5) by $M(1+M\rho)^{(\gamma-3)/2}$ and (6) by M, an addition and a subtraction of the two equations lead to two propagation equations (* is the convolution product):

$$\Big\{\frac{\partial}{\partial t} + (Mu \pm c)\frac{\partial}{\partial x}\Big\}\Big(Mu \pm \frac{2c}{\gamma-1}\Big) = \pm 2MSh\big(1+\frac{\gamma-1}{\sqrt{Pr}}\big)\frac{\partial u}{\partial x} * \frac{1}{\sqrt{\pi t}} + O\big(M^2Sh, MSh^2, \frac{M}{ReSh}\big). \tag{8}$$

These are close to equations obtained by Chester [12] in their dimensionless form.

Two points are different from Chester's equations.

(1) Neglected terms are there evaluated, and appear in the right hand side of equation (8). For example, nonlinearities in the boundary layers are of order (M^2Sh) and the effect of the radius of curvature in the boundary layer is of order (MSh^2). Notice that no terms (M^n) with n integer are neglected: this equation is exact on propagation nonlinearities in the main acoustic field. The evaluation of neglected terms leads to the validity domain of equation (8) (see figure 1).

(2) Volumetric losses are obtained by Chester [12] but do not appear in equation (8). Only thermoviscous losses in the boundary layer should be kept and not volumetric losses (as far as shock waves have not appeared). This conclusion is obtained by the evaluation of order of magnitude of the different terms: volumetric losses (of order (1/Re)) are neglectible compared to other neglected terms such as non linearities in the boundary layers for example (of order (M^2Sh)).

3 Burgers' equations and solutions

3.1 Burgers' equations

Equations (5) and (6) are spatially local equations (on x). But nonlinear phenomena and losses are cumulative: even if effects are locally of order M or Sh, these effects can increase along propagation and can distort the acoustic signal strongly if the tube is long, even if M is small ($M \ll 1$). A classical perturbative calculus to solve equations (5) and (6) is based on an asymptotic expansion, and will not correspond any more to physical problems, because higher terms become too large. An adapted method for cumulative phenomena is necessary: it is the Multiple Scale Method (MSM), which permits a good description of the distortion of the wave until distances $x = O(1/M)$ (distance of order of the critical shock wave distance). M and Sh are considered to be each other of the same order in this part.

$\frac{\partial}{\partial x}$ is replaced by $\frac{\partial}{\partial x} + M\frac{\partial}{\partial X}$ with x the rapid scale and X the slow scale, where $X = Mx$.

An expansion of the variables in the small parameter M is:

$$\rho_a = \rho_{1a} + M\rho_{2a} + O(M^2) \quad P_a = P_{1a} + MP_{2a} + O(M^2) \quad u_a = u_{1a} + Mu_{2a} + O(M^2)$$

The different orders of magnitude are now separated.

Order 0:

Equations (5), (6) and (25) become respectively:

$$\frac{\partial \rho_{1a}}{\partial t} + \frac{\partial u_{1a}}{\partial x} = 0, \quad \frac{\partial u_{1a}}{\partial t} + \frac{\partial \rho_{1a}}{\partial x} = 0 \quad \text{and} \quad P_{1a} = \gamma\rho_{1a},$$

which are the equations of ordinary linear non-dissipative acoustics. They give:

$$\left\{\frac{\partial^2}{\partial t^2} - \frac{\partial^2}{\partial x^2}\right\}(u_{1a}, \rho_{1a}, P_{1a}) = 0.$$

Let us introduce the notation $\theta^+ = t - x$ and $\theta^- = t + x$. Solutions of the equations are at order 0:

$$u_{1a} = q^+(\theta^+, X) - q^-(\theta^-, X), \quad \rho_{1a} = q^+(\theta^+, X) + q^-(\theta^-, X), \quad P_{1a} = \gamma\big(q^+(\theta^+, X) + q^-(\theta^-, X)\big).$$

The order 0 is not enough to make explicit the dependence of q^+ on θ^+ and X, or the dependence of q^- on θ^- and X: it is necessary to continue on to order 1.

Order 1:

Introducing the new dimensionless number $T = Sh\left(1 + \frac{\gamma-1}{\sqrt{Pr}}\right)$, (5) and (6) are in order 1:

$$\frac{\partial \rho_{2a}}{\partial t} + \frac{\partial u_{2a}}{\partial x} = -\frac{\partial}{\partial X}(q^+ - q^-) - 2q^+\frac{\partial q^+}{\partial x} + 2q^-\frac{\partial q^-}{\partial x} + \frac{2T}{M}\frac{\partial}{\partial x}(q^+ - q^-) * \frac{1}{\sqrt{\pi t}}, \tag{9}$$

$$\frac{\partial u_{2a}}{\partial t} + \frac{\partial \rho_{2a}}{\partial x} = -\frac{\partial}{\partial X}(q^+ + q^-) - (\gamma-1)q^+\frac{\partial q^+}{\partial x} - (\gamma-1)q^-\frac{\partial q^-}{\partial x} - (\gamma-3)q^+\frac{\partial q^-}{\partial x} - (\gamma-3)q^-\frac{\partial q^+}{\partial x}, \tag{10}$$

Applying $\frac{\partial}{\partial t}(9) - \frac{\partial}{\partial x}(10)$, and changing variables from (x,t,X) to (θ^+,θ^-,X) leads to:

$$\begin{aligned} 4\frac{\partial^2 \rho_{2a}}{\partial\theta^+\partial\theta^-} = \quad & \tfrac{\partial}{\partial\theta^+}\left((\gamma+1)q^+\tfrac{\partial q^+}{\partial\theta^+} - 2\tfrac{\partial q^+}{\partial X} - 2\tfrac{T}{M}\tfrac{\partial q^+}{\partial\theta^+} * \tfrac{1}{\sqrt{\pi\theta^+}}\right) \\ & + \tfrac{\partial}{\partial\theta^-}\left((\gamma+1)q^-\tfrac{\partial q^-}{\partial\theta^-} + 2\tfrac{\partial q^-}{\partial X} - 2\tfrac{T}{M}\tfrac{\partial q^-}{\partial\theta^-} * \tfrac{1}{\sqrt{\pi\theta^-}}\right) \\ & + (\gamma-3)\left\{\tfrac{\partial}{\partial\theta^+} - \tfrac{\partial}{\partial\theta^-}\right\}^2(q^+q^-). \end{aligned} \tag{11}$$

$$\tag{12}$$

A similar equation satisfied by u_{2a} is obtained from $\frac{\partial}{\partial t}(10) - \frac{\partial}{\partial x}(9)$.

The first term in equation (11) is independent of θ^-. An integration on θ^- would therefore contain a secular term in the expression of ρ_2. The same thing is true for the second term with an integration on θ^+. But the third term is not secular when integrated by θ^+ or θ^-. Secular terms must equal 0 to keep a correct result when non linearities increase. After an integration this leads to (the constant of integration is chosen equal to 0):

$$\frac{\partial q^+}{\partial\sigma} = q^+\frac{\partial q^+}{\partial\theta^+} - \frac{T}{\epsilon}\frac{\partial q^+}{\partial\theta^+} * \frac{1}{\sqrt{\pi\theta^+}} \tag{13}$$

$$\frac{\partial q^-}{\partial\sigma} = -q^-\frac{\partial q^-}{\partial\theta^-} + \frac{T}{\epsilon}\frac{\partial q^-}{\partial\theta^-} * \frac{1}{\sqrt{\pi\theta^-}} \tag{14}$$

$$\text{with} \quad \sigma = \tfrac{\gamma+1}{2}X \quad \text{and} \quad \epsilon = \tfrac{\gamma+1}{2}M.$$

* is the convolution product.

Traveling waves:

If a traveling wave is propagating in the positive x-direction:

$$q^- = 0 \quad \text{and} \quad u_{1a} = \rho_{1a} = \tfrac{1}{\gamma} P_{1a} = q^+(\theta^+, X).$$

q^+ satisfies the single generalized Burgers' equation (13).

This result was obtained by Blackstock [9]. This Burgers' equation does not contain the second-order derivative, which decribes the effect of the volumetric losses. Volumetric losses are negligible as long as the shock wave has not appeared (Sugimoto [14]). It would be necessary to describe the profile of the shock structure of the early portion of the weak shock (Pierce [26]).

Standing waves:

The most important result to be applied to standing waves is the fact that the two Burgers' equations (13) and (14) are independent and the standing wave can therefore be considered as the sum of two independent progressive waves, the incident wave and the reflected wave. The interaction between these two waves exists locally (given by the third term of the equation (11)), but it is not a cumulative phenomenon and it therefore remains negligible. This idea is essential for the resolution of these equations in the following section. Notice that Burgers' equations (13) and (14) are obviously similar if θ^+ and X are changed respectively on θ^- and -X.

3.2 Solution of Burgers' equations

Generalized Burger's equations (13) and (14) have no analytical known solutions. Solutions are therefore done numerically. Solutions are performed in ω-space. Fractional derivative becomes a multiplication by $(j\omega)^{1/2}$.

Traveling waves

The following traveling wave is considered:

$$q = \sum_{n=1}^{+\infty} \left(a_n(\sigma) \sin n\theta + b_n(\sigma) \cos n\theta \right). \tag{15}$$

The nonlinear term of the Burgers' equations is therefore in Fourier series:

$$
\begin{aligned}
q\frac{\partial q}{\partial \theta} &= \Big(\sum_{n=1}^{+\infty}\big(a_n(\sigma)\sin n\theta + b_n(\sigma)\cos n\theta\big)\Big)\Big(\sum_{p=1}^{+\infty}\big(-pb_p(\sigma)\sin p\theta + pa_p(\sigma)\cos p\theta\big)\Big) \\
&= \sum_{m=1}^{+\infty}\Big(m\sin m\theta\Big(\sum_{p=1}^{m-1}\big(\frac{a_p a_{m-p}}{2} - \frac{b_p b_{m-p}}{2}\big) - \sum_{p=m+1}^{+\infty}\big(a_{p-m}a_p + b_{p-m}b_p\big)\Big)\Big) \\
&+ \sum_{m=1}^{+\infty}\Big(m\cos m\theta\Big(\sum_{p=1}^{m-1}\big(\frac{a_p b_{m-p}}{2} + \frac{b_p a_{m-p}}{2}\big) + \sum_{p=m+1}^{+\infty}\big(b_{p-m}a_p - a_{p-m}b_p\big)\Big)\Big)
\end{aligned}
\tag{16}
$$

and the fractional derivative is:

$$
\frac{\partial^{1/2} q}{\partial^{1/2}\theta} = \sum_{m=1}^{+\infty}\sqrt{\frac{m}{2}}\Big((a_m - b_m)\sin m\theta + (a_m + b_m)\cos m\theta\Big). \tag{17}
$$

Equalizing each term of the Fourier series leads to the set of equations:

$$
\begin{cases}
\frac{\partial a_n}{\partial \sigma} = n\Big(\sum_{p=1}^{n-1}\big(\frac{a_p a_{n-p}}{2} - \frac{b_p b_{n-p}}{2}\big) - \sum_{p=n+1}^{+\infty}(a_{p-n}a_p + b_p b_{p-n})\Big) - \frac{T}{\epsilon}\sqrt{\frac{n}{2}}(a_n - b_n) \\
\frac{\partial b_n}{\partial \sigma} = n\Big(\sum_{p=1}^{n-1}\big(\frac{a_p b_{n-p}}{2} + \frac{b_p a_{n-p}}{2}\big) + \sum_{p=n+1}^{+\infty}(b_{p-n}a_p - b_p a_{p-n})\Big) - \frac{T}{\epsilon}\sqrt{\frac{n}{2}}(a_n + b_n)
\end{cases}
$$

These Fourier series are truncated to N harmonics. Then a resolution on σ by small steps $\triangle\sigma$ (finite difference method) knowing the initial condition at $\sigma = 0$ is performed. The resolution method used is a prediction correction method. At first order, the classical method called Euler is used, and correction is performed using the Adams Moulton second order method.

Standing waves

Two boundary conditions are used to solve the two Burgers' equations: the acoustic pressure at the input (E), and pressure or impedance at (S). Everywhere the acoustic signal is considered as the sum of the incoming q+ and the outgoing q- waves. These two periodic waves are assumed to be a Fourier sum of N harmonics. The iterative method is based on a numerical convergence (Newton Raphson method) of the components of q+ towards the solution of a set of nonlinear equations. At each loop, q+ is propagated from (E) to (S) using a finite different approximation of the equation (13) as in the former paragraph. For the first loop, an arbitrary wave q+ at (E) is chosen: the signal of the source for example, or better the incident wave of the linear solution if known. Using the known value of the acoustic pressure at (S), the reflected wave q- is deduced and then propagated from (S) to (E) by applying equation (14). Finally q+ is induced in (E) from the known value of the acoustic pressure at this point. The comparison between the components of q+ at

the beginning and at the end of the loop gives the set of nonlinear equations. A harmonic balance method called Newton-Raphson is used to solve this set of equations, and converges quite rapidly.

Similar solutions are used for nonlinear propagation without losses, or linear propagation with losses. The same Burgers equations are used (and therefore the same numerical resolution), removing respectively the term corresponding to the thermoviscous boundary layer losses or the nonlinearities. It is useful in order to compare the respective effect of these two phenomena on the acoustic wave. The linear solutions are validated with classical known methods. Notice that nonlinear stationary case without losses doesn't converge (losses are necessary for numerical convergence). Obtained nonlinear solutions are compared with Chester's results in the particular case of a closed tube with a rigid termination ($|q^+| = |q^-|$), and lead to quite similar predictions. The main contribution of this work is that these predictions can be applied whatever the termination is, and not only to closed tubes with rigid terminations or open tubes. The following experiments (standing waves part 4-3) are not performed in a particular case but with an unknown termination. This kind of case cannot be predicted by Chester's theory or other classical theories.

Only results in part 4-1 (traveling wave) can be predicted by classical theories.

4 Experiments

4.1 Experimental setup and procedure

Experiments are performed in a cylindrical air-filled tube 6m long and 58mm internal diameter with an absorbing termination. The tube is composed of different sections connected by flanges. Some sections have a port in which a microphone can be mounted. The three microphones used to measure the internal sound pressure level are acceleration compensated piezo-electrical gauges, type PCB M116B. The microphones (8mm external diameter) are mounted flush with the pipe wall. Calibration of each installed microphone involves a reference microphone (B&K model 4138, 1/4 in.) mounted flush in a closed pipe end. This closed pipe end is placed near each microphone from the first one (near the source) to the last one (near the absorbing termination), the complete tube being assembled after the last calibration. The reference microphone is calibrated using a pistonphone B&K 4420. The source is a compression loudspeaker driver, JBL

model 2446H. The loudspeaker output is as close as possible to the tube without contact to minimize wall vibrations. The frequency and the level of the pure harmonic excitation signal is produced by the internal generator of a dual phase lock-in amplifier (type Stanford SR 850). A block diagram of the experimental setup is shown in Fig.4.1.

The procedure is to generate sinusoidal signals at the source ranging from low to high amplitude. For each source level, the amplitude and the phase of the first harmonics from each microphone signal (typically 3) are measured accurately with the lock-in amplifier. The measurements are conducted for two fundamental frequencies : firstly at 2000Hz, secondly at 500Hz. Notice that the cut-off frequency below which the plane wave approximation is valid is around 3300Hz. At 2000Hz the absorbing termination is efficient, the outgoing wave reflected from the end of the tube is negligible, the experimental results are compared with a traveling wave theory (see the following section 4.2). At 500Hz the absorbing termination is not so efficient, the outgoing wave is not negligible, the experimental results are compared with a standing wave theory (see section 4.3).

FIGURE 4.1 Block diagram of the experimental setup. M are microphones (Piezo-electical gauges).

4.2 Traveling wave

As explained in the previous section, a sinusoidal signal at frequency 2000Hz is produced by the source. Two microphone signals are analysed : the first one M1 is near the source, the second one M3 is near the absorbing termination (4.98m from M1). Thirteen measurements are performed for different acoustic levels from 125 to 152dB (amplitude of the first harmonic in M1). Because of the absorbing termination, a purely progressive travelling wave is present in the tube. The nonlinear propagating theory in tubes is checked as follows. The measured pressure in M1 is propagated theoretically as far as the M3 position, and then compared with the measured pressure in M3. The comparison between the calculated and the measured M3 pressure is displayed in the figures 4.2 and 4.3. The calculated pressure is based on the computing procedure

described in section 3. The two measured pressure are defined with their first 3 harmonics (amplitude and phase).

More precisely, in figure 4.2(a), the ratio of the fundamental pressure amplitudes of M3 over M1 are displayed in a decibel scale, as a function of the fundamental pressure amplitude of M1 in a decibel scale (dBSPL). The experimental results are compared with four theoretical results (cases 0, 1, 2 and 3 figure 4.2): (0) the lossless linear propagation case (the straight line equal to 0 dB), (1) the lossless nonlinear propagation case, (2) the lossy linear propagation case (the straight line at -1.95 dB represents attenuation due to the thermoviscous losses near the wall of the tube), (3) the lossy nonlinear propagation case. The theoretical results corresponding to the nonlinear theories, cases (1) and (3), are computed with the method described in section 3. Notice that the lossless case (1) can be directly obtained with the well known Fubini analytical results. To check the validity of the theory when the effect of nonlinear propagation are small and comparable to the thermoviscous effects, a carefully calibration of the microphones and an accurate knowledge of the temperature are essential. The accuracy of the absolute calibration can be estimated as $\pm$0.1dB. Notice that because of the calibration procedure described section 4.1, the relative calibration accuracy between the microphones M3 and M1 is most probably less than 0.1dB. The temperature determination (equivalent to the velocity of sound determination) is estimated in an indirect way : for the lowest source level (125dB SPL) the linear propagation theory is valid. Then the attenuation measurement between M3 and M1 allows the estimation of the temperature. Figure 4.2(a) illustrates particularly well the good agreement between the lossy nonlinear propagation theory based on the generalized Burgers' equation, and the experimental results. Nevertheless, there is a small but significant discrepancy between the theory and the experiment (0.2dB at the largest source sound pressure level 152dB). This systematic discrepancy increasing from 0 to 0.2dB as a function of the source sound pressure level, can be understood according to the accuracy of the calibration of the microphone M1. In figure 4.2(b), the fundamental pressure amplitude of M3 is displayed as a function of the fundamental pressure amplitude of M1 in decibel scales, the experimental results are compared to the theoretical results in the same way as in figure 4.2(a).

FIGURE 4.2(a) and (b) Traveling wave case, first harmonic, dB scale display

For source sound pressure levels higher than 140dB, there are losses on the fundamental due to the nonlinear effects (see figure 4.2), acoustic energy is transfered to higher harmonics: the growth in amplitude of harmonic 2 and harmonic 3 in M3 as a function of the source level increase is presented figure 4.3(b) and figure 4.3(c) respectively; the fundamental amplitude is presented again in figure 4.3(a) (the axes are linear in units of Pascal).

The experimental results are compared with two theoretical results (cases 1 and 3 figure 4.3): (1) the lossless nonlinear propagation case, (3) the lossy nonlinear propagation case. These theoretical results corresponding to the nonlinear theories are computed with the method described in section 3. The figure 4.3(b) illustrates the good agreement between the lossy nonlinear propagation theory based on the generalized Burgers' equation (13), and the experimental results for harmonic 2. The agreement for harmonic 3 is not so good. It is not so surprising, this harmonic corresponding to a frequency of 6000Hz clearly above the cutoff frequency of the tube, the plane wave approximation is not valid anymore. Incidently, theoretical results corresponding to the lossy linear propagation theory (2) are displayed on figures 4.3(b) and (c). These results come from the linear propagation of small components of harmonics 2 and 3 being present in the signal due to the source signal not being perfectly sinusoidal (slight nonlinear behavior of the loudspeaker).

FIGURE 4.3(a)(b) and (c) Traveling wave case, first, second and third harmonics, linear scale display

4.3 Standing wave

A sinusoidal signal at frequency 500Hz is produced by the source. Three microphone signals are analysed: the first one M1 is near the source, the third one M3 is near the absorbing termination (4.98m from M1), the second one M2 is between M1 and M3, 3.955m from M1. Ten measurements are performed for different acoustic levels from 127 to 152dB, 45 to 790 Pa (amplitude of the first harmonic in M1). The three measured

pressures are defined with their first 3 harmonics (amplitude and phase).

At 500Hz, the absorbing termination is less efficient than at 2000Hz, the outgoing wave traveling in the tube has to be taken into account. The experimental results are examined with a stationary wave theory. According to the simulation procedure described in section 3 for the standing wave case, two reference pressure signals are necessary to calculate the pressure field between them. The measured pressure signals in M1 and M3 are the reference, the pressure at the position of M2 is calculated, and then compared with the M2 measured pressure. The comparison between the calculated and the measured M2 pressures is displayed in the figures 4.4 and 4.5.

More precisely, in figure 4.4, the fundamental pressure amplitude of M2 is displayed as a function of the fundamental pressure amplitude of M1 using linear scales (pascal units). The experimental results are compared with three theoretical results (cases 1, 2 and 3 figure 4.4): (1) the lossy nonlinear propagation case, (2) the lossy linear standing wave case, (3) the lossy nonlinear standing wave case. The theoretical results corresponding to the standing theories, cases (2) and (3), are similar and in agreement with the experimental results. The effect of nonlinearities are not noticeable on the fundamental pressure amplitude at 500Hz. Furthermore, the propagative theory is not applicable to this study as was assumed at the beginning of this section (see the discrepancy between the curves (1) and the experimental results figure 4.4).

FIGURE 4.4 Standing wave case, first harmonic, linear scale display

Effects of nonlinearities are noticeable in harmonic 2 of the pressure, they are considered below and displayed figure 4.5. In figure 4.5, the harmonic 2 pressure amplitude of M2 is displayed as a function of the fundamental pressure amplitude of M1 using linear scales (pascal units). The experimental results are compared with three theoretical results (cases 1, 2 and 3 figure 4.5): (1) the lossy nonlinear propagation case, (2) the lossy linear standing wave case, (3) the lossy nonlinear standing wave case. These theoretical results are computed with the method described in section 3. Figure 4.5 illustrates good agreement between the

lossy nonlinear standing wave theory, case (3), and the experimental results for harmonic 2. Having a look at the discrepancy between curves (2) and the experimental results figure 4.5, the effects of nonlinearities are noticeable on harmonic 2 of the pressure. It is confirmed that the propagative theory is not applicable to this study (see the discrepancy between the curves (1) and the experimental results figure 4.5).

FIGURE 4.5 Standing wave case, second harmonic, linear scale display

5 Closing remarks

The propagation of finite-amplitude plane waves in a cylindrical air-filled tube has been investigated between 10 and 3000Hz for levels of 140-160dB, in the case of weakly nonlinear propagation. The analysis separates cumulative effects which increase with propagation distance and lead to important distortion of the signal, and non cumulative effects which depend on the order of M and Sh. In order to simplify the resolution, non cumulative effects are neglected: the accuracy of the theoretical results may therefore be of order M and Sh. This theory is valid as long as a shock has not formed and for any boundary conditions (the wave needs not be purely propagating or stationary).

The experimental findings confirm the theoretical predictions developed in this paper. Experiments are performed up to 152dB (the limit of the electro-acoustic source), and errors remain of order of 0.1dB on the fundamental and the harmonic number 2. Notice that the highest sound levels of the experiments correspond to $M \sim 10^{-2}$: neglected non cumulative effects are therefore of order of 1% (0.1dB), corresponding to the order of magnitude of the discrepancy between the predictions and the experiments.

A Setting of non linear equations of propagation

A.1 Main acoustic field equations

A.1.1 Non dimensional equations

The conservation laws (1), (2) and (3) are written in cylindrical coordinates. The angular coordinate is ignored. Dimensionless variables defined in the main acoustic field are inserted. γ is the specific heat ratio for a gas.

The mass conservation law becomes:

$$\frac{\partial \rho_a}{\partial t} + \frac{\partial}{\partial x}\Big((1+M\rho_a)u_a\Big) + (1+M\rho_a)Sh\frac{1}{r_1}\frac{\partial}{\partial r_1}(r_1 v_a) + \frac{M}{Re}v_a\frac{\partial \rho_a}{\partial r_{b2}} = 0. \tag{18}$$

The axial component of the momentum conservation law is:

$$(1+M\rho_a)\frac{\partial u_a}{\partial t} + (1+M\rho_a)M\Big(u_a\frac{\partial u_a}{\partial x} + \frac{1}{Re}v_a\frac{\partial u_a}{\partial r_{b2}}\Big) + \frac{1}{\gamma}\frac{\partial P_a}{\partial x} = \tag{19}$$

$$(\frac{1}{Re})^2\frac{\partial {u_a}^2}{\partial r_{b2}^2} + \frac{Sh}{Re}\frac{1}{r_1}\frac{\partial u_a}{\partial r_{b2}} + \frac{1}{Re}(\frac{\eta}{\mu}+\frac{4}{3})\frac{\partial^2 u_a}{\partial x^2} + \frac{Sh}{Re}(\frac{\eta}{\mu}+\frac{1}{3})\frac{1}{r_1}\frac{\partial}{\partial r_1}(r_1\frac{\partial v_a}{\partial x})$$

and the radial component is:

$$(1+M\rho_a)\frac{\partial v_a}{\partial t} + (1+M\rho_a)M\Big(u_a\frac{\partial v_a}{\partial x} + Shv_a\frac{\partial v_a}{\partial r_1}\Big) + \frac{1}{\gamma}\frac{\partial P_a}{\partial r_{b2}} = \tag{20}$$

$$Sh^2(\frac{\eta}{\mu}+\frac{4}{3})\frac{\partial}{\partial r_1}\Big(\frac{1}{r_1}\frac{\partial}{\partial r_1}(r_1 v_a)\Big) + \frac{1}{Re}(\frac{\eta}{\mu}+\frac{1}{3})\frac{\partial^2 u_a}{\partial r_{b2}\partial x} + (\frac{1}{Re})\frac{\partial^2 v_a}{\partial x^2}.$$

Coming from the energy conservation, the equation of entropy is:

$$\frac{1}{\gamma}(1+M\rho_a)(1+MT_a)\Big(\langle\frac{\partial S_a}{\partial t}\rangle + Mu_a\langle\frac{\partial S_a}{\partial x}\rangle + \frac{1}{Re}Mv_a\langle\frac{\partial S_a}{\partial r_{b1}}\rangle\Big) = \tag{21}$$

$$\frac{1}{(\gamma-1)Pr}\Big(\big(\frac{1}{Re}\big)^2\frac{\partial^2 T_a}{\partial r_{b2}^2} + \frac{Sh}{Re}\frac{1}{r_1}\frac{\partial T_a}{\partial r_{b2}} + \frac{1}{Re}\frac{\partial^2 T_a}{\partial x^2}\Big) + \frac{M}{Re}\big(\frac{\eta}{\mu}+\frac{4}{3}\big)\big(\frac{\partial u_a}{\partial x}\big)^2 + \frac{M}{Re^2}\Big(\big(\frac{\partial v_a}{\partial x}\big)^2 + \big(\frac{\partial u_a}{\partial r_{b2}}\big)^2\Big)$$

$$+\frac{MSh}{Re}\Big(\big(\frac{\eta}{\mu}-\frac{2}{3}\big)\frac{\partial u_a}{\partial x}\big(\frac{\partial v_a}{\partial r_1}+\frac{1}{r_1}\frac{\partial(r_1 v_a)}{r_1}\big)\Big) + \frac{MSh^2}{Re}\Big(2(\frac{\partial v_a}{\partial r_1})^2 + \big(\frac{\eta}{\mu}-\frac{2}{3}\big)\frac{\partial v_a}{\partial r_1}\frac{1}{r_1}\frac{\partial(r_1 v_a)}{\partial r_1}\Big).$$

Gas is perfect:

$$(1+MP_a) = (1+M\rho_a)(1+MT_a) \quad \text{therefore} \quad P_a = \rho_a + T_a + M\rho_a T_a. \tag{22}$$

According to the state principle, the local thermodynamic state is fixed by any two independent thermodynamic variables. It implies for a perfect gas:

$$dS_a = \big(\frac{\gamma}{\gamma-1}\big)\frac{dT_a}{1+MT_a} - \frac{dP_a}{1+MP_a} \quad \text{or} \quad dS_a = -\big(\frac{\gamma}{\gamma-1}\big)\frac{d\rho_a}{1+M\rho_a} + \big(\frac{1}{\gamma-1}\big)\frac{dP_a}{1+MP_a}. \tag{23}$$

A.1.2 Leading orders

The equation of entropy is written at leading order:

$$\frac{1}{\gamma}\langle\frac{\partial S_a}{\partial t}\rangle = \frac{1}{(\gamma-1)Pr}\big(\frac{1}{Re}\big)\frac{\partial^2 T_a}{\partial x^2}.$$

Variation of the entropic term is of order $1/Re$ in the main acoustic field. This is the adiabatic hypothesis valid up to the order 2 (order 0, 1 and 2 on M and Sh) which leads to (using (23)):

$$\big(\frac{\gamma}{\gamma-1}\big)\frac{dT_a}{1+MT_a} = \frac{dP_a}{1+MP_a} + O\big(\frac{1}{Re}\big), \tag{24}$$

as well as

$$(1+MP_a) = (1+M\rho_a)^\gamma + O\big(\frac{1}{Re}\big) \quad \text{and} \quad \frac{\partial P_a}{\partial x} = \gamma(1+M\rho_a)^{\gamma-1}\frac{\partial \rho_a}{\partial x} + O\big(\frac{1}{Re}\big). \tag{25}$$

From the equations (18) and (19) ((19) divided by $(1+M\rho_a)$), we get an expansion in small parameters M and Sh. Order 0 and 1 on M and Sh leads to dimensionless conservation of mass and momentum:

$$\frac{\partial \rho_a}{\partial t} + \frac{\partial}{\partial x}\big((1+M\rho_a)u_a\big) + Sh\frac{1}{r_1}\frac{\partial}{\partial r_1}(r_1 v_a) = O\big(MSh, \frac{M}{Re}\big), \tag{26}$$

$$\frac{\partial u_a}{\partial t} + Mu_a\frac{\partial u_a}{\partial x} + \frac{1}{\gamma}\frac{1}{(1+M\rho_a)}\frac{\partial P_a}{\partial x} = O\big(\frac{1}{Re}\big). \tag{27}$$

Equation (27) is written with variables u_a, v_a and ρ_a with the help of (25):

$$\frac{\partial u_a}{\partial t} + Mu_a\frac{\partial u_a}{\partial x} + (1+M\rho_a)^{\gamma-2}\frac{\partial \rho_a}{\partial x} = O\big(\frac{1}{Re}\big). \tag{28}$$

Nonlinear equations in the main acoustic field are the set of two equations (26) and (28) depending on variables u_a and ρ_a, and on variable v_a which will be used to match the boundary layer. The matching term is $\left(Sh\frac{1}{r_1}\frac{\partial}{\partial r_1}(r_1 v_a)\right)$ (of order Sh): v_a will be calculated only at order 0. This justify the fact that boundary layers can be considered as linear in our conditions. The following calculations in the boundary layer are therefore given at order 0 only.

Notice that the only usefulness of equation (20) is to check the coherence between the scales of $\tilde{v}_a$ and radial variations of $\tilde{P}_a$ (when writing (20) at order 0).

A.2 Boundary layer equations

A.2.1 Non dimensional equations

The conservation laws (1), (2) and (3) are written in cylindrical coordinates. Dimensionless variables defined in the acoustic boundary layer are inserted.

The mass conservation law is:

$$\frac{\partial \rho_{ab}}{\partial t} + \frac{\partial}{\partial x}\Big((1+M\rho_{ab})u_{ab}\Big) + \frac{\partial}{\partial r_{b1}}\Big((1+M\rho_{ab})v_{ab}\Big) + Sh\frac{1}{r_1}(1+M\rho_{ab})v_{ab} = 0. \tag{29}$$

The axial component of momentum conservation is

$$(1+M\rho_{ab})\frac{\partial u_{ab}}{\partial t} + (1+M\rho_{ab})M\Big(u_{ab}\frac{\partial u_{ab}}{\partial x} + v_{ab}\frac{\partial u_{ab}}{\partial r_{b1}}\Big) + \frac{1}{\gamma}\frac{\partial P_{ab}}{\partial x} = \tag{30}$$
$$\frac{\partial {u_{ab}}^2}{\partial r_{b1}^2} + Sh\frac{1}{r_1}\frac{\partial u_{ab}}{\partial r_{b1}} + \frac{1}{Re}(\frac{\eta}{\mu}+\frac{4}{3})\frac{\partial^2 u_{ab}}{\partial x^2} + \frac{1}{Re}(\frac{\eta}{\mu}+\frac{1}{3})\frac{\partial^2 v_{ab}}{\partial r_{b1}\partial x} + \Big(\frac{Sh}{Re}\Big)(\frac{\eta}{\mu}+\frac{1}{3})\frac{1}{r_1}\frac{\partial v_{ab}}{\partial x},$$

and the radial component is

$$(1+M\rho_{ab})\frac{\partial v_{ab}}{\partial t} + (1+M\rho_{ab})M\Big(u_{ab}\frac{\partial v_{ab}}{\partial x} + v_{ab}\frac{\partial v_{ab}}{\partial r_{b1}}\Big) + \frac{1}{\gamma}\frac{\partial P_{ab}}{\partial r_{b2}} = \tag{31}$$
$$(\frac{\eta}{\mu}+\frac{4}{3})(\frac{\partial^2 v_{ab}}{\partial r_{b1}^2} + Sh\frac{1}{r_1}\frac{\partial v_{ab}}{\partial r_{b1}} - Sh^2\frac{1}{r_1^2}v_{ab}) + (\frac{\eta}{\mu}+\frac{1}{3})\frac{\partial^2 u_{ab}}{\partial r_{b1}\partial x} + \frac{1}{Re}\frac{\partial^2 v_{ab}}{\partial x^2}.$$

Coming from energy conservation, the equation of entropy is:

$$\frac{1}{\gamma}(1+M\rho_{ab})(1+MT_{ab})\Big(\langle\frac{\partial S_{ab}}{\partial t}\rangle + Mu_{ab}\langle\frac{\partial S_{ab}}{\partial x}\rangle + Mv_{ab}\langle\frac{\partial S_{ab}}{\partial r_{b1}}\rangle\Big) = \tag{32}$$
$$\frac{1}{(\gamma-1)Pr}\Big(\frac{\partial^2 T_{ab}}{\partial r_{b1}^2} + Sh\frac{1}{r_1}\frac{\partial T_{ab}}{\partial r_{b1}} + \frac{1}{Re}\frac{\partial^2 T_{ab}}{\partial x^2}\Big) + M\big(\frac{\partial u_{ab}}{\partial r_{b1}}\big)^2 + \frac{M}{Re}\Big(\big(\frac{\eta}{\mu}+\frac{4}{3}\big)\big(\frac{\partial u_{ab}}{\partial x}\big)^2 + 2\big(\frac{\partial v_{ab}}{\partial r_{b1}}\big)^2$$
$$+\big(\frac{\eta}{\mu}-\frac{2}{3}\big)\frac{\partial u_{ab}}{\partial x}\big(\frac{\partial v_{ab}}{\partial r_{b1}} + \frac{1}{r_1}\frac{\partial(r_1 v_{ab})}{r_1}\big) + \big(\frac{\eta}{\mu}-\frac{2}{3}\big)\frac{\partial v_{ab}}{\partial r_1}\Big(\frac{1}{r_1}\frac{\partial(r_1 v_{ab})}{\partial r_{b1}}\Big)\Big) + M\big(\frac{1}{Re}\big)^2\big(\frac{\partial {v_{ab}}^2}{\partial x}\big).$$

The perfect gas equation and thermodynamic bivariance are not changed from the main acoustic field equations (22) and (23).

A.2.2 Order 0

The equation of entropy (32) points out that variations of S are of order of unity in the boundary layer: isentropy would not be valid there.

We get an expansion in the small parameters M, Sh and $1/Re$. At order 0, conservation laws (29), (30), (32) and thermodynamic equations respectively lead to:

$$\frac{\partial \rho_{ab}}{\partial t} + \frac{\partial u_{ab}}{\partial x} + \frac{\partial v_{ab}}{\partial r_{b1}} = O(M, Sh), \tag{33}$$

$$\frac{\partial u_{ab}}{\partial t} + \frac{1}{\gamma}\frac{\partial P_{ab}}{\partial x} = \frac{\partial^2 u_{ab}}{\partial r_{b1}^2} + O\big(M, Sh, \frac{1}{Re}\big), \tag{34}$$

$$\frac{1}{\gamma}\frac{\partial S_{ab}}{\partial t} = \frac{1}{(\gamma-1)Pr}\frac{\partial^2 T_{ab}}{\partial r_{b1}^2} + O\big(M, Sh, \frac{1}{Re}\big), \tag{35}$$

$$dS_{ab} = \big(\frac{\gamma}{\gamma-1}\big)dT_{ab} - dP_{ab} \tag{36}$$

$$P_{ab} = \rho_{ab} + T_{ab} + O(M). \tag{37}$$

This set of equations will be used to calculate the acoustic signal in the boundary layer verifying boundary conditions.

A.3 Asymptotic matching

A.3.1 Spatial averaging

Acoustic quantities are quasi-uniform across a section of the tube in the main acoustic field. To obtain a spatially one dimensional problem, equations in the main acoustic field are averaged across a section of the tube. The average is written:

$$\overline{X} = \frac{1}{S}\int\int_S X dS. \tag{38}$$

Equations (26) and (28) become:

$$\frac{\partial \overline{\rho_a}}{\partial t} + \frac{\partial}{\partial x}\big(\overline{(1+M\rho_a)u_a}\big) + Sh\overline{\frac{1}{r_1}\frac{\partial}{\partial r_1}(r_1 v_a)} = O\big(MSh, \frac{M}{Re}\big), \tag{39}$$

$$\frac{\partial \overline{u_a}}{\partial t} + M\overline{u_a\frac{\partial u_a}{\partial x}} + \overline{(1+M\rho_a)^{\gamma-2}\frac{\partial \rho_a}{\partial x}} = O\big(\frac{1}{Re}\big). \tag{40}$$

Stokes formula imply

$$\int\int_S \frac{1}{r}\frac{\partial}{\partial r}(rf)dS = \oint_\Gamma f dl. \tag{41}$$

Applied to v_a, it leads to:

$$\overline{\frac{1}{r_1}\frac{\partial}{\partial r_1}(r_1 v_a)dS} = \frac{1}{S}\int\int_S \frac{1}{r_1}\frac{\partial}{\partial r_1}(r_1 v_a)dS = \frac{1}{S}\oint_\Gamma v_a dl = \frac{\Gamma}{S}v_L. \tag{42}$$

v_L is the radial velocity component at the interface between the boundary layer and the main acoustic field. Γ is the dimensionless perimeter and S the dimensionless surface of a section. Γ/S depends on the geometry of the tube. For a cylinder:

$$\frac{\Gamma}{S} = \frac{\frac{1}{R}2\pi R}{\frac{1}{R^2}\pi R^2} = 2. \tag{43}$$

v_L is determined by asymptotic matching with the boundary layer. Variation of acoustic dimensionless variables across a section in the main field is of order 1/(ReSh). To replace the value at any point along a radius with the cross section average implies an approximation of order 1/(ReSh). Equations (39) and (40) can therefore be written:

$$\frac{\partial \rho_a}{\partial t} + \frac{\partial}{\partial x}\big((1+M\rho_a)u_a\big) + 2Shv_L = O\big(MSh, \frac{1}{ReSh}\big), \tag{44}$$

$$\frac{\partial u_a}{\partial t} + Mu_a\frac{\partial u_a}{\partial x} + (1+M\rho_a)^{\gamma-2}\frac{\partial \rho_a}{\partial x} = O\big(\frac{1}{ReSh}\big). \tag{45}$$

A.3.2 The asymptotic matching velocity in the boundary layer

The aim of this paragraph is to write explicitly the velocity v_L, the asymptotic value of the radial component v_{ab} of the acoustic velocity in the boundary layer. Energy conservation (35) and the thermodynamic equation (36) lead to:

$$\frac{\partial T_{ab}}{\partial t} - \big(\frac{\gamma-1}{\gamma}\big)\frac{\partial P_{ab}}{\partial t} = \frac{1}{Pr}\frac{\partial^2 T_{ab}}{\partial r_{b1}^2} + O\big(M, Sh, \frac{1}{Re}\big) \tag{46}$$

Let us write indexed acoustic values ρ_a, P_a, T_a and u_a averaged across a section in the main acoustic field (they depend only on x and t), and let us expand variables as following:

$$\rho_{ab} = \rho_a + \rho_b, \quad T_{ab} = T_a + T_b, \quad P_{ab} = P_a + P_b, \quad u_{ab} = u_a + u_b.$$

Variation of P_a and P_{ab} is respectively across the section of the main acoustic field (1/ReSh), and across the boundary layer (1/Re) (according to dimensional analysis in part 1). It implies $P_{ab} = P_a + O(1/ReSh)$ and equation of perfect gas (22) is in the boundary layer:

$$P_a = \rho_a + \rho_b + T_a + T_b + O\big(M, \frac{1}{ReSh}\big)$$

and in the main acoustic field:

$$P_a = \rho_a + T_a + O(M),$$

therefore

$$\rho_b = -T_b + O\big(M, \frac{1}{ReSh}\big). \tag{47}$$

The same arguments with equations of conservation of momentum (27) and (34) lead to, after a subtraction:

$$\frac{\partial u_b}{\partial t} = \frac{\partial^2 u_b}{\partial r_{b1}^2} + O(M, Sh, \frac{1}{ReSh}), \tag{48}$$

and by addition of equations of entropy (24) and (35) (with the help of (36)):

$$\frac{\partial T_b}{\partial t} = \frac{1}{Pr}\frac{\partial^2 T_b}{\partial r_{b1}^2} + O(M, Sh, \frac{1}{ReSh}), \tag{49}$$

and by subtraction of equations of conservation of mass (26) and (33):

$$\frac{\partial \rho_b}{\partial t} + \frac{\partial u_b}{\partial x} + \frac{\partial v_{ab}}{\partial r_{b1}} = O(M, Sh). \tag{50}$$

Equations (48) and (49) are solved taking into account the boundary layer conditions. In order to simplify the resolution, r_{b1} is replaced with r', with r'=0 at the tube wall and positive inside:

$$r' = \frac{1}{\xi}(R - \tilde{r}) = \frac{R}{\xi} - r_{b1}.$$

These conditions are at $r' = 0$:

$$u_b = -u_a, \quad T_b = -T_a, \tag{51}$$

and according to the asymptotic matching method, for $r' \to \infty$

$$u_b \longrightarrow 0, \quad T_b \longrightarrow 0. \tag{52}$$

Equations (48), (49) and (50) are converted in ω-space to be solved.

The solutions of the equations (48) and (49) are:

$$u_b = -u_a(x,\omega)\exp\big(-\sqrt{i\omega}r'\big) + O\big(M, Sh, \frac{1}{ReSh}\big), \tag{53}$$

$$T_b = -T_a(x,\omega)\exp\big(-\sqrt{i\omega}\sqrt{Pr}r'\big) + O\big(M, Sh, \frac{1}{ReSh}\big). \tag{54}$$

Equation (50) is:

$$i\omega\rho_b + \frac{\partial u_b}{\partial x} + \frac{\partial v_{ab}}{\partial r_{b1}} = O(M, Sh). \tag{55}$$

Using (53) and (54), an integration on r_{b1} of equation (50) leads to:

$$v_{ab} = \frac{\gamma-1}{\sqrt{Pr}}\frac{(-1)}{\sqrt{i\omega}}\frac{\partial u_a}{\partial x}\Big(\exp(-\sqrt{i\omega}\sqrt{Pr}r') - 1\Big) + \frac{(-1)}{\sqrt{i\omega}}\frac{\partial u_a}{\partial x}\Big(\exp(-\sqrt{i\omega}r' - 1\Big) + O\big(M, Sh, \frac{1}{ReSh}\big). \quad (56)$$

The velocity v_L is the asymptotic value of v_{ab} at $r' \longrightarrow \infty$. Expressed with r_{b1} instead of r' and in t-space, the result is equivalent to that obtained by Chester [12] (* is the convolution product):

$$v_L = -\Big(1 + \frac{\gamma-1}{\sqrt{Pr}}\Big)\frac{\partial u_a}{\partial x} * \frac{1}{\sqrt{\pi t}} + O\big(M, Sh, \frac{1}{ReSh}\big). \quad (57)$$

This velocity can be written in the equivalent following form:

$$v_L = -\Big(1 + \frac{\gamma-1}{\sqrt{Pr}}\Big)\frac{\partial^{-1/2}}{\partial t^{-1/2}}\Big[\frac{\partial u_a}{\partial x}\Big] + O\big(M, Sh, \frac{1}{ReSh}\big). \quad (58)$$

A.3.3 Nonlinear equations of propagation

Equations (44), (45) and (57) are a set of three equations with three variables. To replace the velocity v_L in the equation (44) leads to the two following equations with only two variables u_a and ρ_a:

$$\frac{\partial \rho_a}{\partial t} + \frac{\partial}{\partial x}\big((1 + M\rho_a)u_a\big) - 2Sh\Big(1 + \frac{\gamma-1}{\sqrt{Pr}}\Big)\frac{\partial u_a}{\partial x} * \frac{1}{\sqrt{\pi t}} = O\big(MSh, Sh^2, \frac{1}{ReSh}\big), \quad (59)$$

$$\frac{\partial u_a}{\partial t} + Mu_a\frac{\partial u_a}{\partial x} + (1 + M\rho_a)^{\gamma-2}\frac{\partial \rho_a}{\partial x} = O\big(\frac{1}{ReSh}\big). \quad (60)$$

Acknowledgments

The authors thank R. Burvingt, F. Coulouvrat and V. Gusev for useful discussions.

References

[1] KIRSCHHOFF G.

Uber den Einfluss der Wärmeleitung in einem gas auf die Schalbewegung [in german]

Poggendorfen Annalen

134

1868

177-193

[2] ZWICKKER G. and KOSTEN C.

Sound absorbing materials

Elsevier

Amsterdam

1949

[3] CRIGHTON D.G.

Nonlinear acoustics, in Modern Methods in analytical acoustics (lecture notes)

Springer-Verlag

London

1992

pp.648-670.

[4] MAKAROV S., OCHMANN M.

Nonlinear and thermoviscous phenomena in acoustics, Part II

Acustica

83

1997

197-222.

[5] HIRSCHBERG A., GILBERT J., MSALLAM R., WIJNANDS A.P.J.

Shock waves in trombones

J. Acoust. Soc. Am.

99 (3)

1996

1754-1758.

[6] GILBERT J. and PETIOT J.F. 1997

Brass instruments, some theoretical and experimental results

In Proceedings of the Institut of Acoustics, ISMA 97

Edinburgh

1997

[7] WHITHAM G.B.

On the propagation of weak shock waves

J. Fluid Mech.

1

1956

290-318

[8] KUZNETSOV V.P.

Equations of nonlinear acoustics

Sov. Phys. Acoust.

19

1971

467-470

[9] BLACKSTOCK D.T.

Nonlinear acoustics (theoretical), in American Institute of Physics Handbook

Mac Graw Hill

New York

1972

3rd ed. Chap. 3n

pp.183-205.

[10] RUDENKO O.V. and SOLUYAN S.I.

Theoretical fundations of nonlinear acoustics

Consultant Bureau

New York

1977

[11] COULOUVRAT F.

On the equations of nonlinear acoustics

J. d'Acoustique

5

1992

321-359.

[12] CHESTER W.

Resonant oscillations in closed tubes

J. Fluid. Mech

18

1964

44-64.

[13] PERNET D.F. and PEYNE R.C.

Non-linear propagation of signals in air

J. Sound Vib. 17 (3)

1971

383-396.

[14] SUGIMOTO N.

Burgers equations with a fractional derivative; hereditary effects on nonlinear acoustic waves

J. Fluid Mech.

225

1991

631-651.

[15] CHESTER W.

Resonant oscillations of a gas in an open-ended tube

Proc. R. Soc. Lond.

A377

1981

449-497.

[16] BLACKSTOCK D.T.

Generalized Burgers equations for plane waves

J. Acoust. Soc. Am.

77 (6)

1985

2050-2053

[17] CRUIKSHANK D.B.

Experimental investigation of finite-amplitude acoustics oscillations in a closed tube

J. Acoust. Soc. Am.

vol.52

1972

1024-1036.

[18] STURTEVANT B.

Nonlinear gas oscillations in pipes, Part 2. Experiments

J. Fluid Mech.

63

1974

97-120

[19] ZARIPOV R.G. and ILHAMOV M.A.

Non-linear gas oscillations in a pipe

J. Sound Vib.

46 (2)

1976

245-257.

[20] GAETE-GARRETON L. and GALLEGO-JUAREZ J.A.

Propagation of finite-amplitude ultrasonic waves in air-II. Plane waves in a tube

J. Acoust. Soc. Am.

73 (3)

1983

768-773.

[21] MAA D-Y. and LIU K.

Nonlinear standing waves: Theory and experiments

J. Acoust. Soc. Am.

98 (5)

1995

2753-2763.

[22] MENGUY L., DURRIEU P. and GILBERT J.

Propagation acoustique non-linéaire dans les guides cylindriques, théorie et résultats expérimentaux préliminaires [text in french]

Actes du 13ième Congrès Français de Mécanique

Poitiers

1997

Vol.1

11-14.

[23] LANDAU L.D. and LIFSCHITZ E.M.

Fluid Mechanics

Pergamon

1959

[24] BATCHELOR G.K.

An introduction to fluid dynamics

Cambridge Univ. Press

Cambridge.

1970

[25] DISSELHORST J.H.M and VAN WIJNGAARDEN L.

Flow in the exit of open pipes during acoustic resonance

J. Fluid Mech.

99 (2)

1980

293-319

[26] PIERCE A.D.

Nonlinear effects in sound propagation, in Acoustics-an introduction to its physical principles and application

Acoust. Soc. Am.

New York

1989

pp.566-615.

FIGURE 1. Validity domain of the theoretical results. The tube radius is 3cm. Each line represents the limit of predominace of one term over an other. The vertical line is the limit of the plane wave approximation. Merkli gives the condition for laminar flow.

FIGURE 4.1. Block diagram of the experimental setup. M are microphones (Piezo-electrical gauges)

FIGURE 4.2. Traveling wave case.

(a) Ratio of the fundamental pressure amplitudes of M3 over M1 (dB scale display), as a function of the fundamental pressure amplitude of M1 (dB scale display).

(b) Fundamental pressure amplitude of M3 (dB scale display) as a function of the fundamental of M1 (dB scale display).

Experimental results ($\diamond$) are compared with four theoretical results:

(0) Lossless linear propagative case;

(1) Lossles nonlinear propagative case;

(2) Lossy linear propagative case;

(3) Lossy nonlinear propagative case.

FIGURE 4.3. Traveling wave case.

First harmonic (a), second harmonic (b) and third harmonic (c) pressure amplitudes of M3 (linear scale display), as a function of the fundamental pressure amplitude of M1 (linear scale display).

Experimental results ($\diamond$) are compared with three theoretical results:

(1) Lossless nonlinear propagative case;

(2) Lossy linear propagative case;

(3) Lossy nonlinear propagative case.

FIGURE 4.4. Stationary wave case.

First harmonic pressure amplitude of M3 (linear scale display), as a function of the fundamental pressure

amplitude of M1 (linear scale display).

Experimental results ($\diamond$) are compared with three theoretical results:

(1) Lossy nonlinear propagative case;

(2) Lossy linear stationary case;

(3) Lossy nonlinear stationary case.

FIGURE 4.5. Stationary wave case.

Second harmonic pressure amplitude of M3 (linear scale display), as a function of the fundamental pressure amplitude of M1 (linear scale display).

Experimental results ($\diamond$) are compared with three theoretical results:

(1) Lossy nonlinear propagative case;

(2) Lossy linear stationary case;

(3) Lossy nonlinear stationary case.

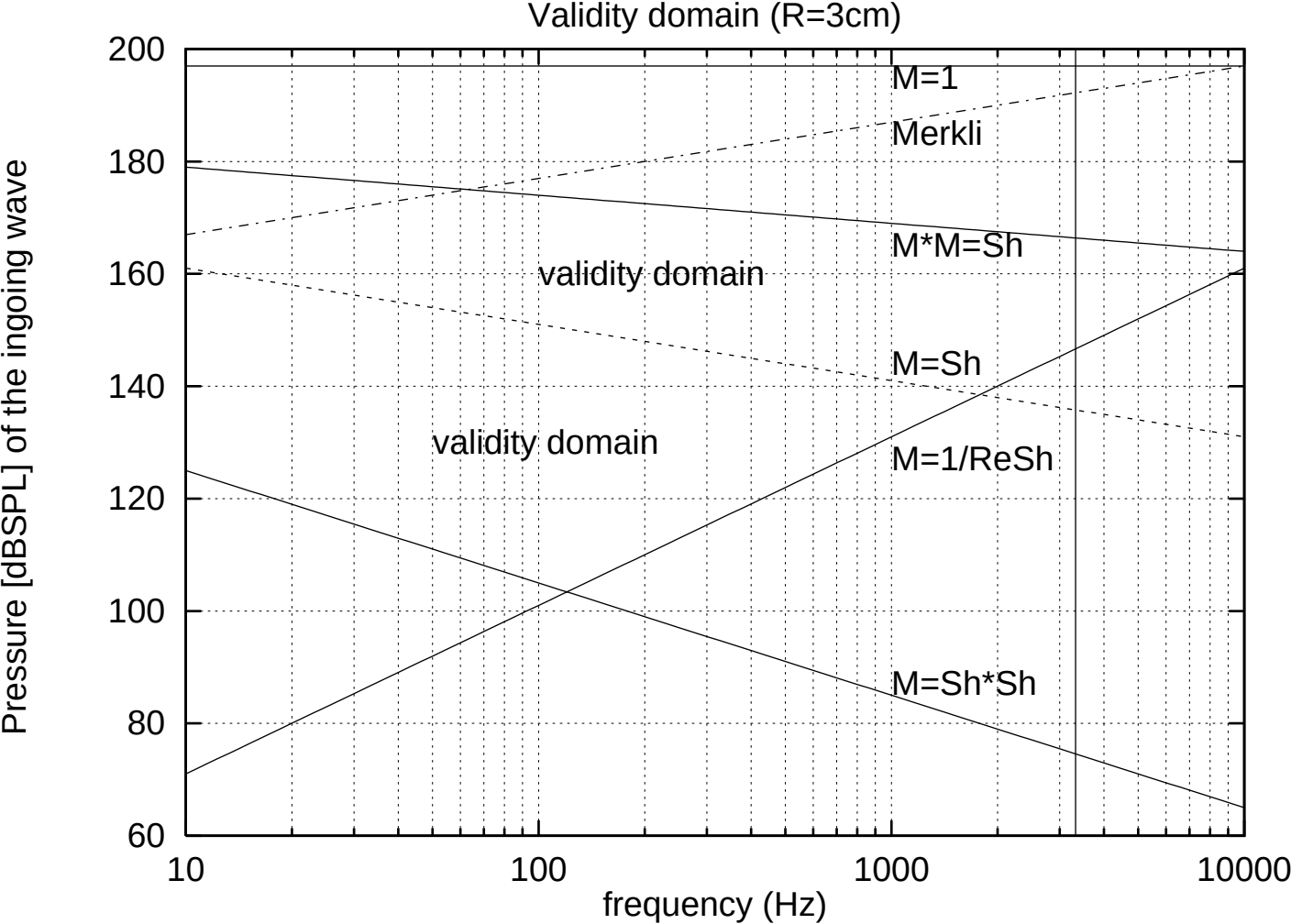
Validity domain (R=3cm)
Pressure [dBSPL] of the ingoing wave
frequency (Hz)
200
180
160
140
120
100
80
60
10
100
1000
10000
M=1
Merkli
M*M=Sh
validity domain
M=Sh
validity domain
M=1/ReSh
M=Sh*Sh

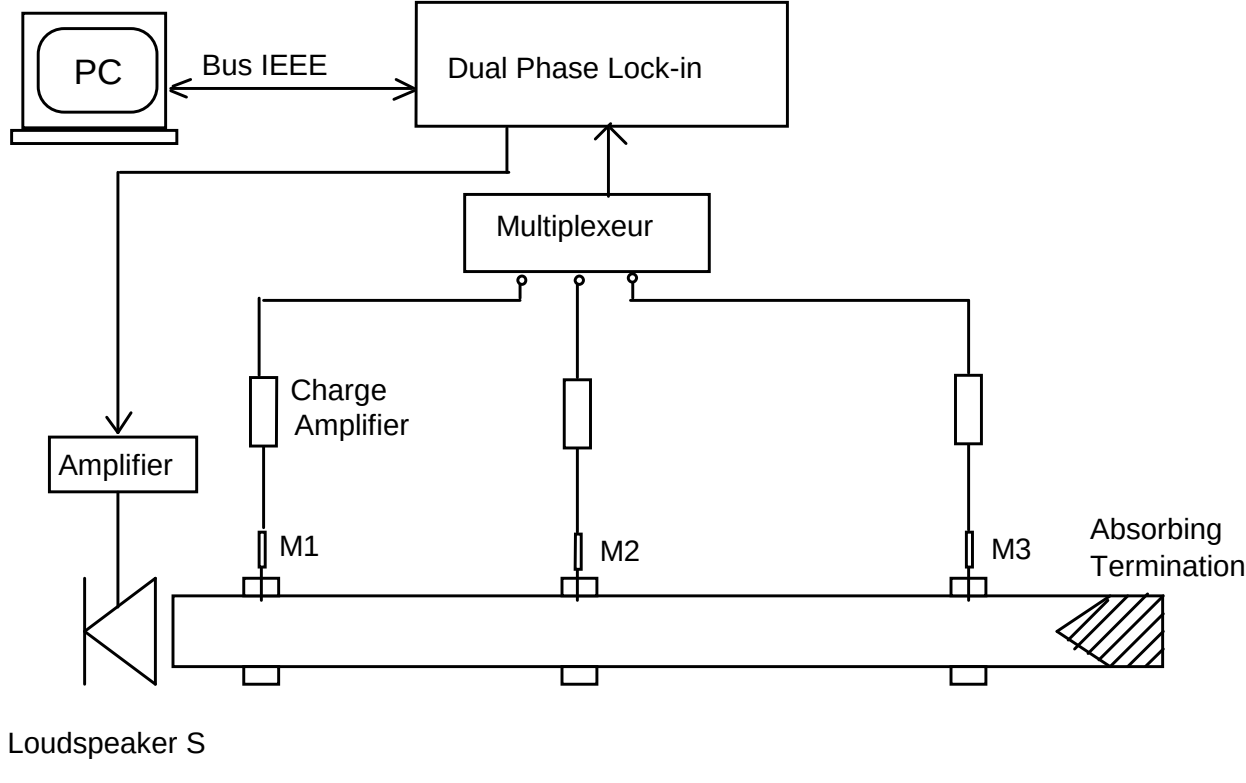
PC
Bus IEEE
Dual Phase Lock-in
Multiplexeur
Charge
Amplifier
Amplifier
M1
M2
M3
Absorbing
Termination
Loudspeaker S

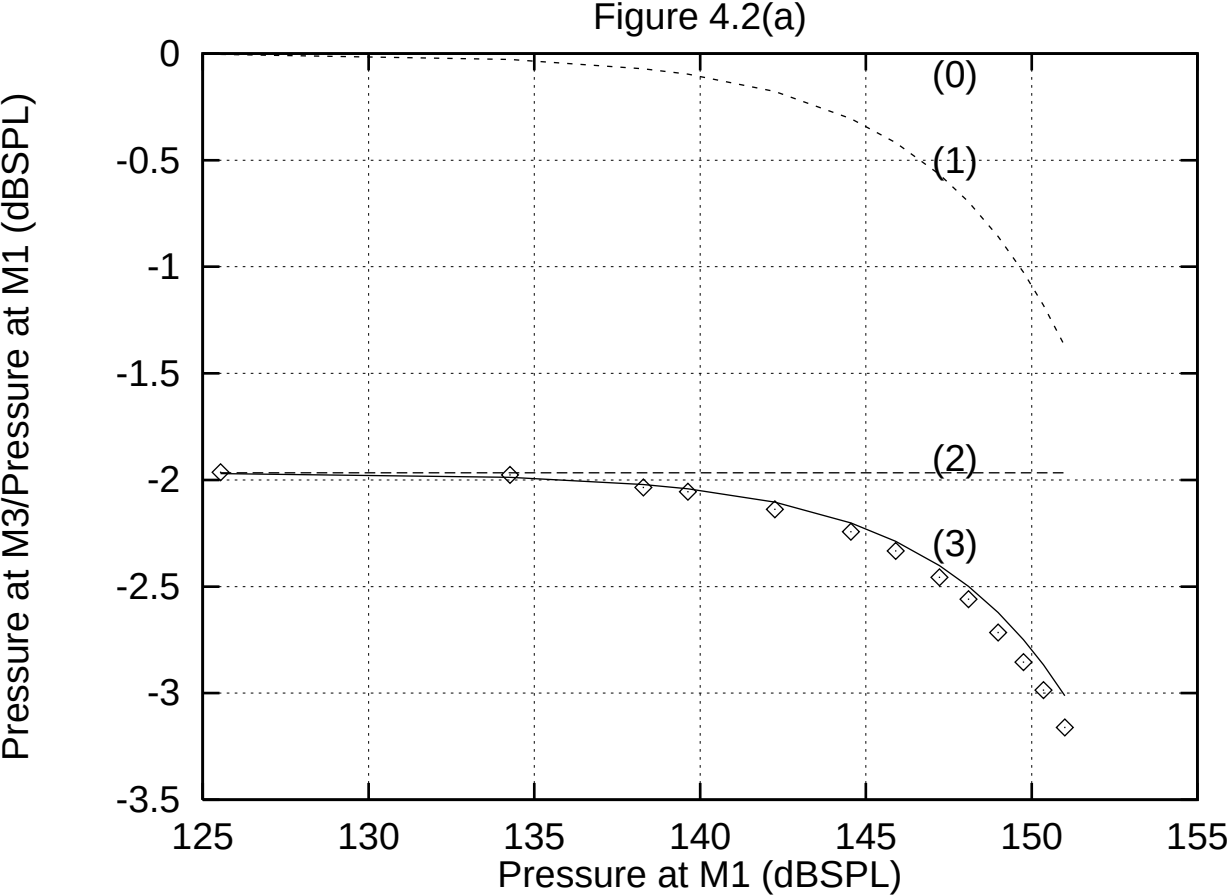
Figure 4.2(a)
0
-0.5
-1
-1.5
-2
-2.5
-3
-3.5
125
130
135
140
145
150
155
Pressure at M3/Pressure at M1 (dBSPL)
Pressure at M1 (dBSPL)
(0)
(1)
(2)
(3)

Figure 4.2(b)

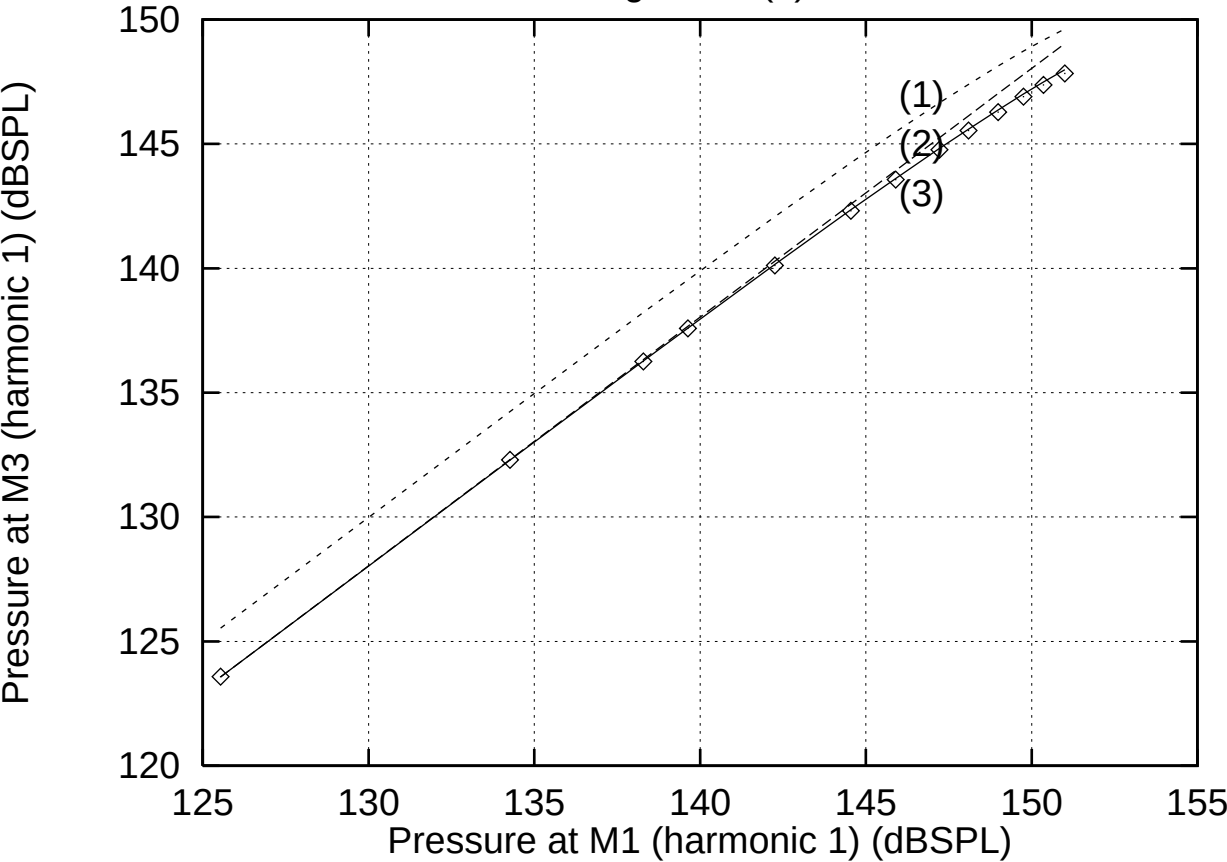
150
145
140
135
130
125
120
125
130
135
140
145
150
155
(1)
(2)
(3)
Pressure at M3 (harmonic 1) (dBSPL)
Pressure at M1 (harmonic 1) (dBSPL)

Figure 4.3.(a)

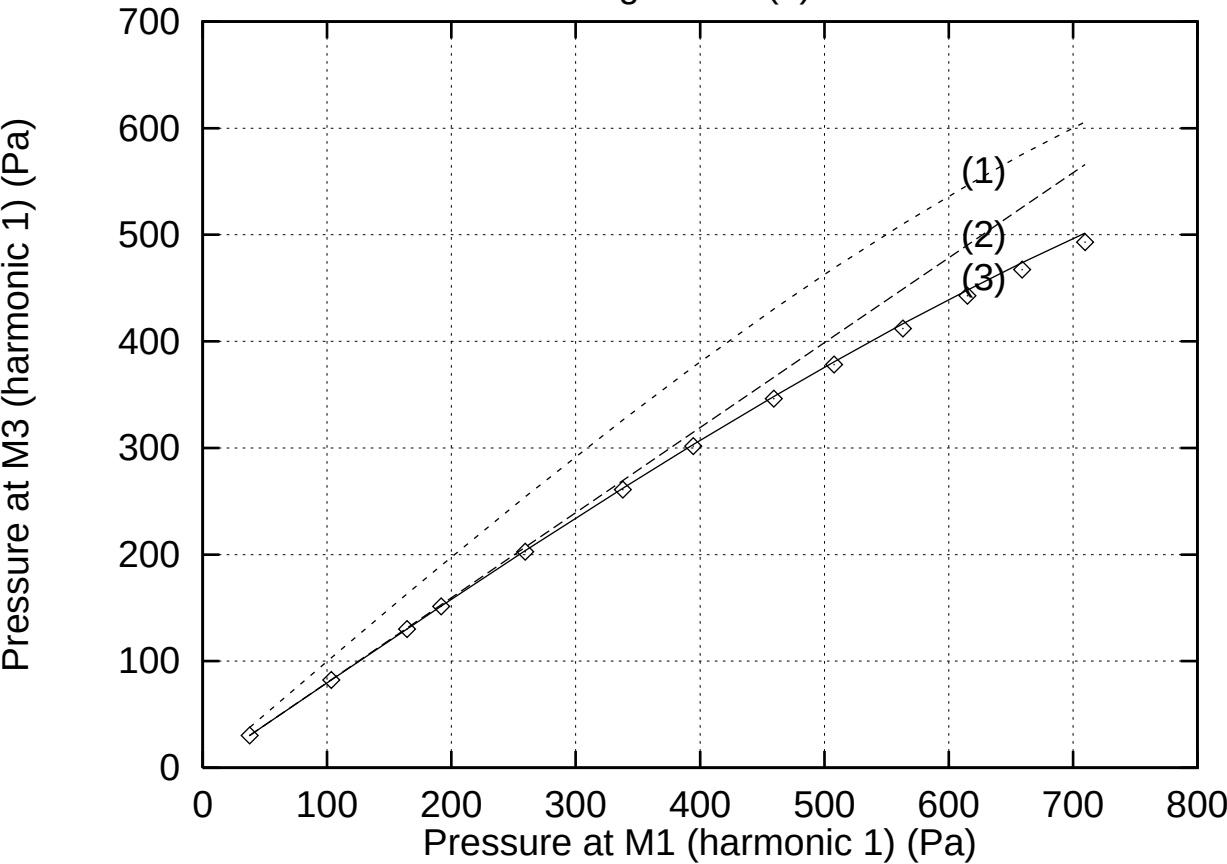
700
600
500
400
300
200
100
0
0
100
200
300
400
500
600
700
800
Pressure at M3 (harmonic 1) (Pa)
Pressure at M1 (harmonic 1) (Pa)
(1)
(2)
(3)

Figure 4.3(b)

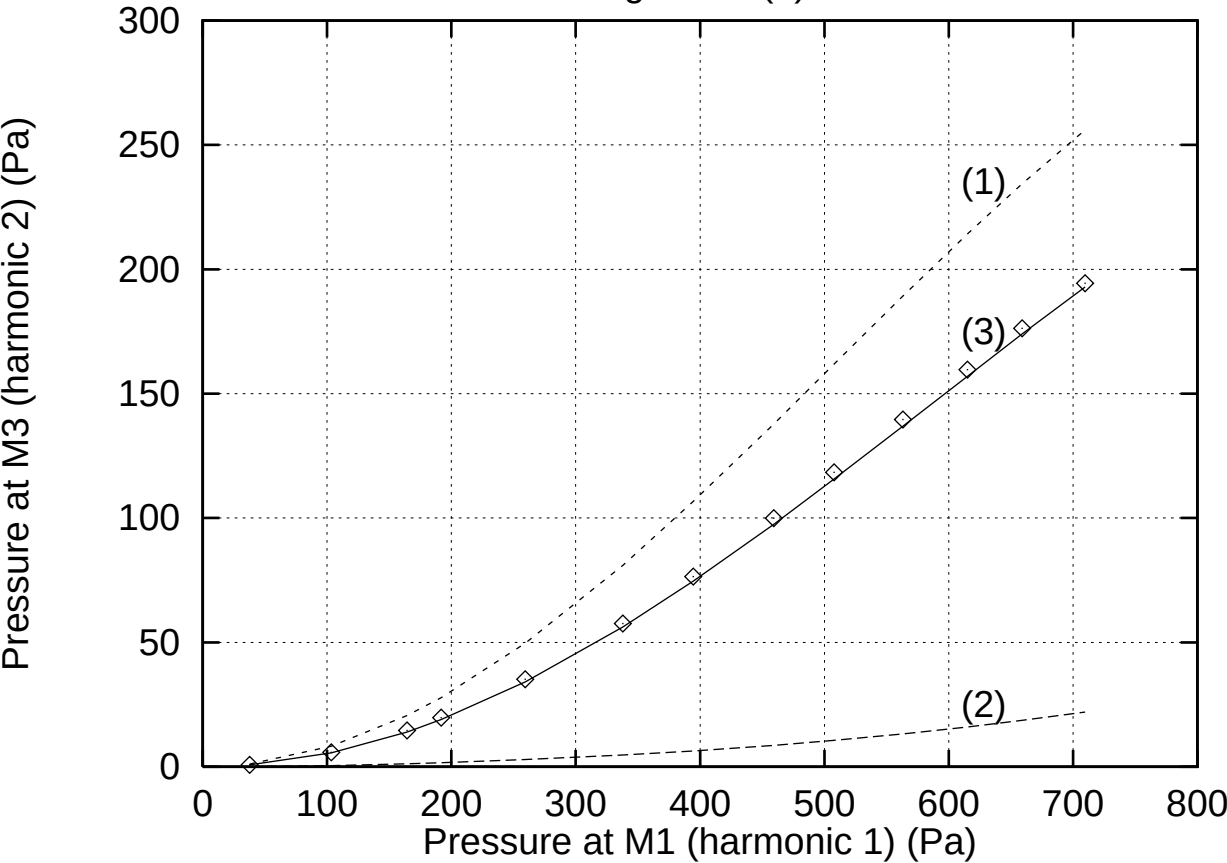
300
250
200
150
100
50
0
0
100
200
300
400
500
600
700
800
Pressure at M3 (harmonic 2) (Pa)
Pressure at M1 (harmonic 1) (Pa)
(1)
(2)
(3)

Figure 4.3(c)

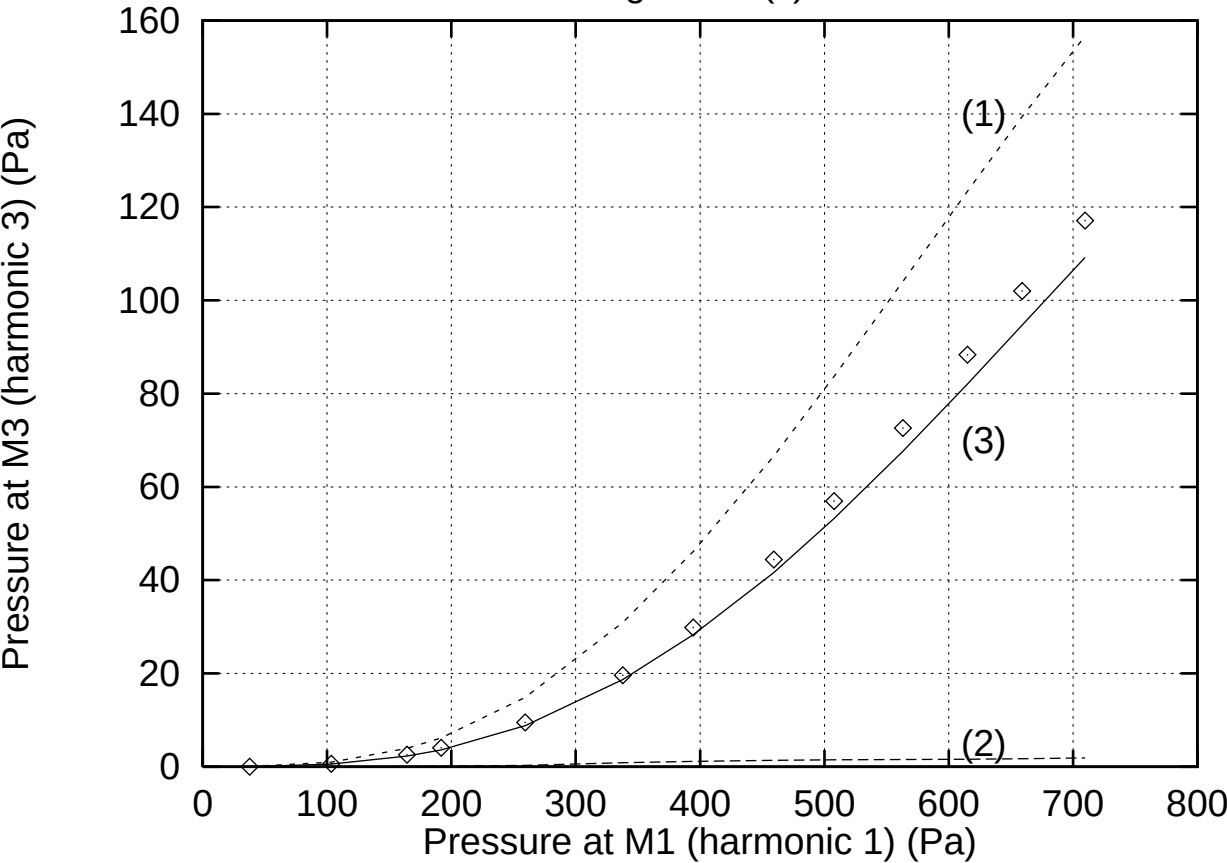
160
140
120
100
80
60
40
20
0
0
100
200
300
400
500
600
700
800
Pressure at M3 (harmonic 3) (Pa)
Pressure at M1 (harmonic 1) (Pa)
(1)
(3)
(2)

Figure 4.4

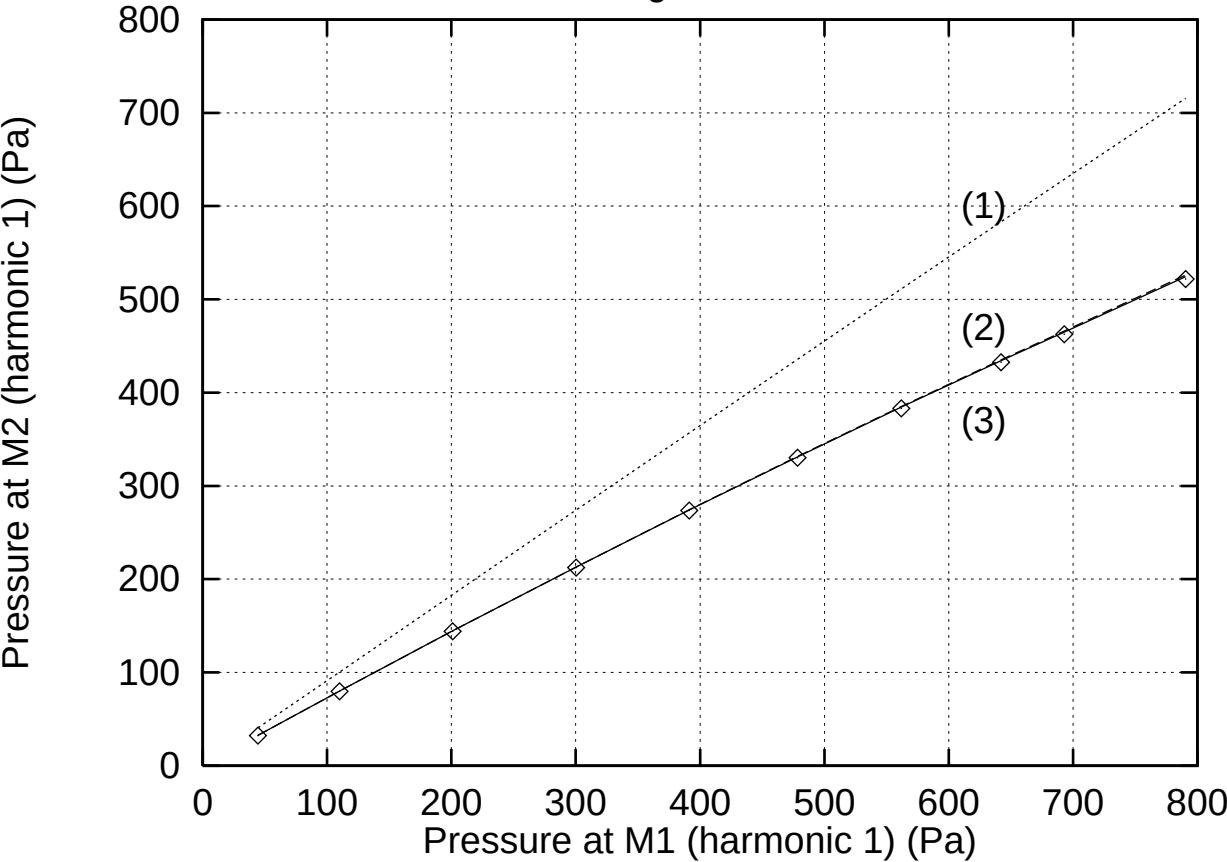
800
700
600
500
400
300
200
100
0
0
100
200
300
400
500
600
700
800
Pressure at M2 (harmonic 1) (Pa)
Pressure at M1 (harmonic 1) (Pa)
(1)
(2)
(3)

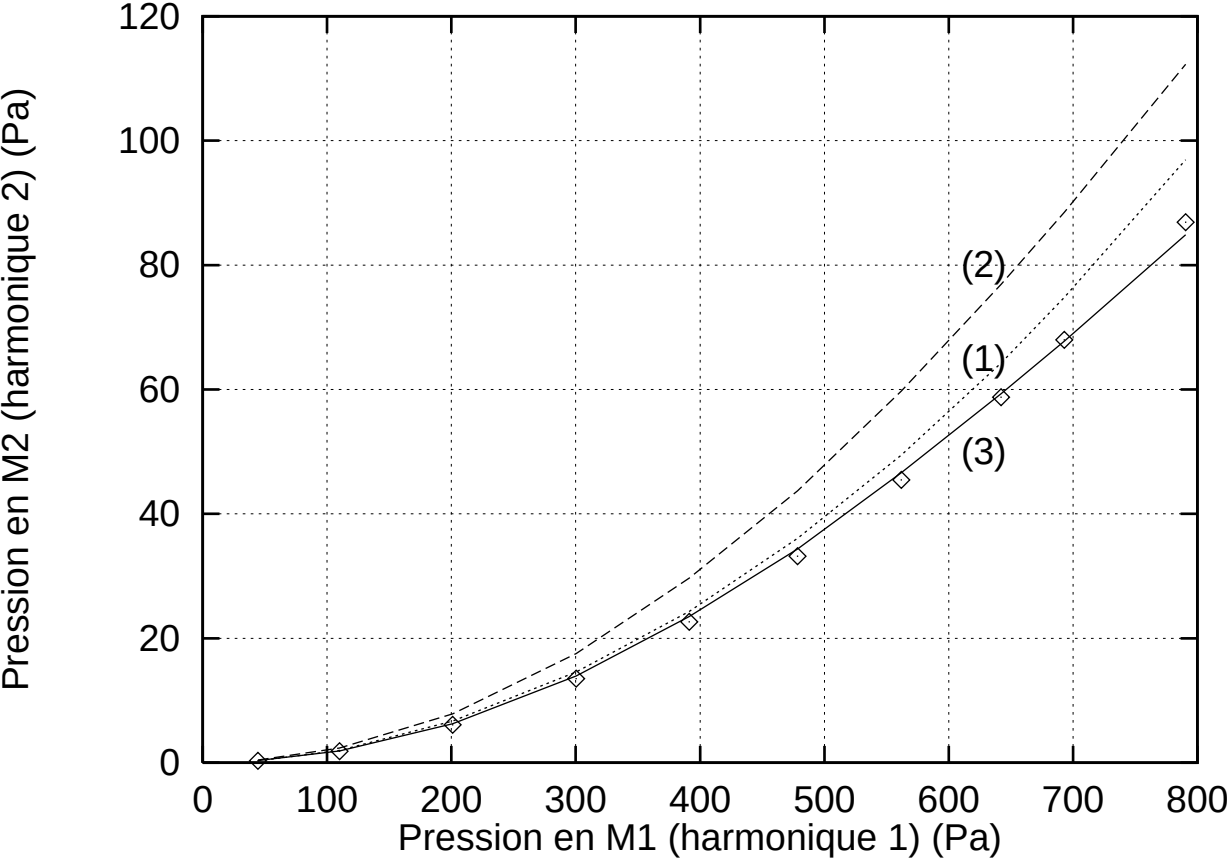
Pression en M2 (harmonique 2) (Pa)
120
100
80
60
40
20
0
0
100
200
300
400
500
600
700
800
Pression en M1 (harmonique 1) (Pa)
(2)
(1)
(3)